

INVERSE MODELLING OF TWO-DIMENSIONAL WATER INFILTRATION INTO A SAND CONTAINING MACROPORES

ADAM SZYMKIEWICZ

Institute of Hydroengineering of the Polish Academy of Sciences, 80328 Gdańsk, Poland,
e-mail: adams@ibwpan.gda.pl

JOLANTA LEWANDOWSKA

Laboratoire Sols, Solides, Structures-Risques (3S- R), BP 53, 38041 Grenoble, France.

RAFAEL ANGULO-JARAMILLO

Laboratoire d'étude des Transferts en Hydrologie et Environnement (LTHE),
BP 53, 38041 Grenoble, France.
Laboratoire des Sciences de l'Environnement, ENTPE, Rue Maurice Audin,
69518 Vaulx-en-Velin, France.

PASCALE LUTZ

Département Géosciences, Institut Polytechnique Lasalle Beauvais, 13 bd. de l'Hautil,
95092 Cergy cedex, France.

Abstract: Two series of axisymmetric laboratory infiltration experiments were carried out in homogeneous sand and in sand containing artificially made vertical macropores. In the first case, the results are compared with numerical solution of the Richards equation. In the second case, the results are compared with the double-porosity model obtained by homogenization. The constitutive relations between the capillary pressure, saturation and unsaturated hydraulic conductivity for the sand and macropores are identified via numerical inverse analysis of cumulative infiltration. The applicability of several types of constitutive functions available in the literature is tested. The saturated conductivity and air-entry pressure fitted for the macropores are compared with theoretical predictions. The cumulative infiltration curves fitted by numerical inversion show reasonable agreement with observations for both types of porous media.

1. INTRODUCTION

The presence of macropores in soil may result from various processes, e.g., shrinkage, plant growth, or soil fauna activity. These large, open pores are activated when the soil approaches full saturation (soil water pressure head close to zero), leading to accelerated infiltration and pollutant transfer. Under drier conditions, water usually does not enter macropores due to their relatively large diameters and they can be treated as impermeable. The flow with active macropores can be described by a double-porosity model based on the homogenization approach, proposed by LEWANDOWSKA et al. [3]. It

consists of a macroscopic-scale equation for the flow in the highly conductive macropores coupled with a set of equations describing local-scale water diffusion from macropores into the sand matrix. A generalized numerical implementation of the model, suitable also for the case of inactive macropores, is presented by SZYMKIEWICZ and LEWANDOWSKA [9]. The model requires the knowledge of the hydraulic functions (i.e., the relations between the capillary pressure, saturation and conductivity), which usually involve 2 to 6 parameters for each sub-domain. In practice, the functions' parameters often have to be identified using inverse methods.

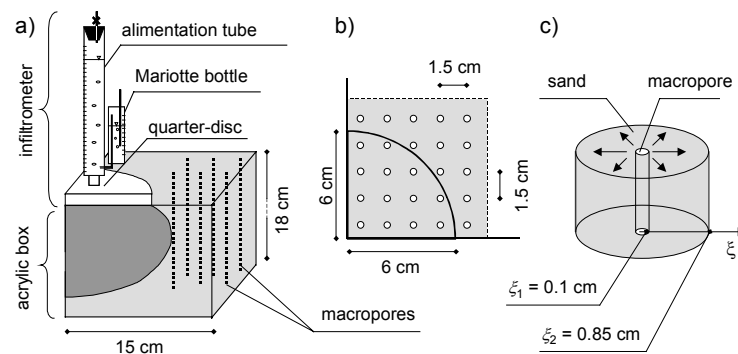


Fig. 1. Experimental setup (a), arrangement of macropores near the infiltrometer disc (b), representation of the local-scale water transfer (c)

In this paper, we present inverse modelling of two series of axisymmetric infiltration experiments performed on homogeneous sand and on sand with macropores, respectively (LUTZ [5]). The analysis was performed in two stages. First, we used the experiments on homogeneous sand to identify the hydraulic functions of the sand by solving inverse problem for the Richards equation. Several types of hydraulic functions were examined. In the second stage, we attempted to reproduce the experiments on sand with macropores using the double-porosity model (SZYMKIEWICZ and LEWANDOWSKA [9]). The sand matrix was characterized by the previously identified parameters. The parameters of macropores were found by solving the inverse problem for the double-porosity model. They were compared with the parameters predicted theoretically on the basis of the macropore geometry.

2. EXPERIMENTS

The experimental setup consisted of an acrylic box of the dimensions of $15 \text{ cm} \times 15 \text{ cm} \times 18 \text{ cm}$ and a quarter tension disc infiltrometer (figure 1a). The infiltrometer with a quarter-disc base of 6 cm radius was positioned at the soil surface in one of the corners of the box. This allowed us to impose a constant negative water pressure head

at the surface. In the first series of tests, the box was filled with weakly compacted sand (Hostun S31). The mean porosity in 10 experiments was 0.495 with standard deviation of 0.015. The mean initial water content was 0.089 with standard deviation of 0.006. The values of the applied surface pressure head h_{surf} were -7 , -4 , -2 , -0.5 and 0 cm (two tests were carried out for each value). The measured cumulative amount of infiltrating water is presented in figure 2a. For each value of h_{surf} we show the results of the two tests and their averages.

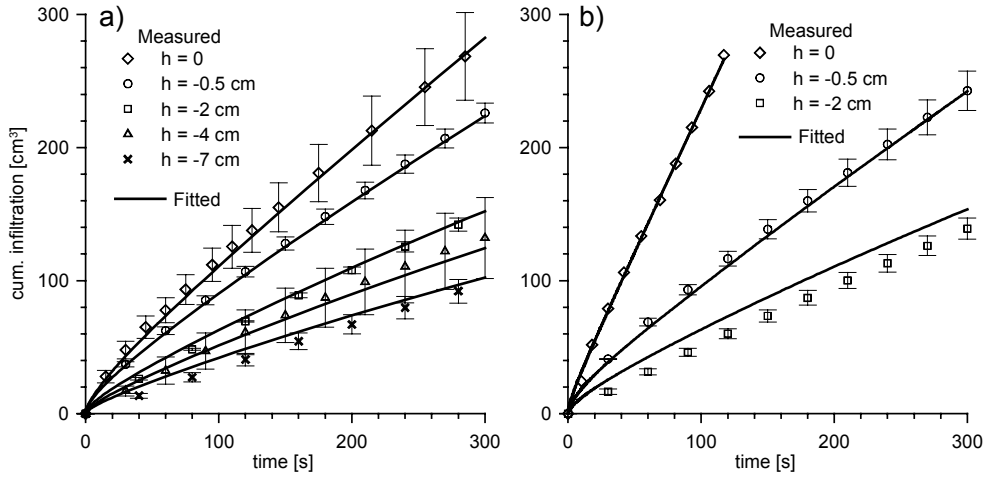


Fig. 2. Measured and fitted cumulative infiltration curves: homogeneous sand (a), sand with macropores (b)

The second series of tests was performed on sand with artificially created macropores. The macropores were made using steel pins of 2 mm in diameter, in regular spacing of 1.5 cm (figure 1b), resulting in the relative volumetric fractions $w_1 = 0.991$ and $w_2 = 0.009$ for the sand matrix and macropores, respectively. The porosity of the sand (not counting macropores) and the initial water content were the same as in the first series. Two experiments were performed for $h_{\text{surf}} = -2$ and -0.5 cm, and one experiment was performed for $h_{\text{surf}} = 0$. The measured cumulative infiltration curves are shown in figure 2b. Note that a significant acceleration of the infiltration rate is observed for $h_{\text{surf}} = 0$.

3. GOVERNING EQUATIONS

3.1. HOMOGENEOUS SAND

We assume that the infiltration in homogeneous sand can be treated as an axisymmetric process, described by the Richards equation in the following form:

$$\frac{\partial \theta_1(h)}{\partial t} - \frac{\partial}{\partial r} \left(K_1(h) \frac{\partial h}{\partial r} \right) - \frac{K_1(h)}{r} \frac{\partial h}{\partial r} - \frac{\partial}{\partial z} \left(K_1(h) \frac{\partial h}{\partial z} - K_1(h) \right) = 0, \quad (1)$$

where: t – the time, r – the radial coordinate, z – the vertical coordinate, θ_1 – the volumetric water content, h – the water pressure head and K_1 – the hydraulic conductivity.

3.2. SAND WITH MACROPORES

When the macropores are active, they form the primary conductive system. The water pressure equilibrates much faster in the macropores than in the sand matrix and thus radial local-scale water transfer between the two systems is observed (figure 1c). In order to capture these non-equilibrium effects, we used the following generalized model for flow in double-porosity media (SZYMKIEWICZ and LEWANDOWSKA [9]):

$$w_1 \frac{\partial \bar{\theta}_1}{\partial t} + w_2 \frac{\partial \theta_2(h)}{\partial t} - \frac{\partial}{\partial r} \left(K_r^{\text{eff}}(h) \frac{\partial h}{\partial r} \right) - \frac{K_r^{\text{eff}}(h)}{r} \frac{\partial h}{\partial r} - \frac{\partial}{\partial z} \left(K_z^{\text{eff}}(h) \frac{\partial h}{\partial z} - K_z^{\text{eff}}(h) \right) = 0, \quad (2)$$

where: w_1, w_2 – the volumetric fractions of the sand and macropores, h – the macroscopic pressure head (corresponding to the macropores), $\bar{\theta}_1$ – the average water content in the sand at a given macroscopic point (r, z) , θ_2 – the water content in macropores, $K_r^{\text{eff}}, K_z^{\text{eff}}$ – the effective conductivity of the medium in radial and vertical directions, respectively. The local-scale flow at an arbitrary macroscopic point (r, z) is assumed to be radial (figure 1c) and is described by the following equation:

$$\frac{\partial \theta_1(h_1)}{\partial t} - \frac{\partial}{\partial \xi} \left(K_1(h_1) \frac{\partial h_1}{\partial \xi} \right) - \frac{K_1(h_1)}{\xi} \frac{\partial h_1}{\partial \xi} = 0 \quad (3)$$

with the boundary conditions: $h_1 = h$ at $\xi = \xi_1$ and $\partial h_1 / \partial \xi = 0$ at $\xi = \xi_2$, where ξ – the local radial coordinate, ξ_1 – the macropore radius, ξ_2 – the radius of the soil mantle, h_1 – the local-scale pressure head in sand. The effective conductivity depends on the conductivities of the two porous systems and their geometry. For the particular arrangement of macropores considered here the conductivity in horizontal direction can be obtained using the Hashin–Shtrikman formula (LEWANDOWSKA et al. [4]), while the conductivity in vertical direction is given by weighted arithmetic mean:

$$K_r^{\text{eff}}(h) = K_1(h) + \frac{2w_2 K_1(h)(K_2(h) - K_1(h))}{2K_1(h) + w_1(K_2(h) - K_1(h))}, \quad (4a)$$

$$K_z^{\text{eff}}(h) = w_1 K_1(h) + w_2 K_2(h). \quad (4b)$$

The model (2)–(4) remains valid also for lower values of h_{surf} , when the macropores are practically impermeable and in the equilibrium with the sand matrix (SZYMKIEWICZ and LEWANDOWSKA [9]).

Equations (1) and (2)–(3) were solved numerically with the DPOR-2D code developed by the authors, based on a fully implicit finite volume formulation (SZYMKIEWICZ et al. [10]). The solution domain represents a quarter of cylinder with $0 \leq z \leq 18$ cm and $0 \leq r \leq 16.93$ cm, which has the same volume as the box. A constant pressure head is imposed at a part of the upper boundary ($0 \leq r \leq 6$ cm), while the other boundaries are treated as impermeable.

4. INVERSE ANALYSIS

4.1. HOMOGENEOUS SAND

We attempted to reproduce the experiments in homogeneous sand using a few well-known types of hydraulic functions. They are expressed in terms of the effective water saturation S_E , defined as $S_E = (\theta - \theta_R)/(\theta_S - \theta_R)$, where θ_S and θ_R denote the water content at saturation and the residual water content, respectively. The van GENUCHTEN [11] functions (VG) have the following form:

$$S_E(h) = (1 + (h/h_g)^n)^{-m}, \quad (5a)$$

$$K(h) = K_S S_E^a (1 - (1 - S_E^{1/m})^m)^b, \quad (5b)$$

where h_g , n – the soil-dependent parameters and K_S – the conductivity at saturation. If MUALEM's [6] (M) conductivity model is applied, $m = 1 - 1/n$, $a = 0.5$ and $b = 2$, while for BURDINE's [2] (B) model $m = 1 - 2/n$, $a = 2$ and $b = 1$. The BROOKS and COREY [1] functions (BC) are:

$$S_E(h) = (h_a/h)^\lambda, \quad (6a)$$

$$K(h) = K_S S_E^\eta, \quad (6b)$$

where h_a – the air entry pressure, λ , η – dimensionless exponents. Equations (6a,b) are valid for $h < h_a$, while for $h \geq h_a$, $S_E = 1$ and $K = K_S$. The exponent η is defined as $\eta = 2.5/\lambda$ for the Mualem's model and $\eta = 3/\lambda$ for the Burdine's model. It is also possible to treat η as an independent parameter and use the function (6b) with any type of the $S_E(h)$ relation (5a or 6a).

Seven sets of hydraulic functions were examined. Four of them represent the standard models: VG-M, VG-B, BC-M, BC-B. The other three sets include the conduc-

tivity function given by equation (6a) with independent parameter η combined with various retention functions: (5a) with $m = 1-1/n$ (VG1- η), (5a) with $m = 1-2/n$ (VG2- η) and (6a) (BC- η). In order to solve the inverse problem, we defined the objective function as the sum of squared errors (SSQ) between the observed and predicted cumulative infiltration. The search for the parameter set which minimizes the objective function was carried out using the Marquardt–Levenberg algorithm (PRESS et al. [7]). In order to reduce the number of fitted parameters, we assumed that $\theta_R = 0$ and $\theta_S = 0.495$ (i.e., equal to the porosity).

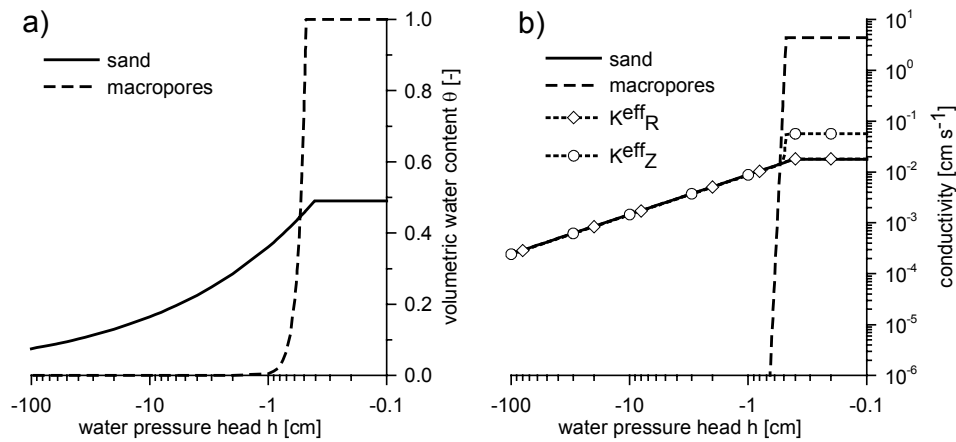


Fig. 3. Retention (a) and conductivity (b) functions fitted for sand and macropores and the effective conductivity functions

Table

Parameters fitted for homogeneous sand using various hydraulic functions

Functions	K_S [cm s ⁻¹]	$h_g(h_a)$ [cm]	n (λ) [-]	η [-]	SSQ [cm ⁶]
VG-M	1.88×10^{-2}	-18.18	1.34	–	1.47×10^4
VG-B	1.96×10^{-2}	-11.05	2.18	–	1.86×10^4
BC-M	1.24×10^{-2}	-0.37	0.14	–	1.37×10^6
BC-B	1.66×10^{-2}	-0.38	0.14	–	1.41×10^6
VG1- η	2.04×10^{-2}	-0.67	1.32	3.08	2.63×10^3
VG2- η	1.88×10^{-2}	-0.49	2.32	2.82	2.08×10^3
BC- η	1.78×10^{-2}	-0.41	0.34	2.29	1.90×10^3

The table lists the fitted values of the parameters and the resulting value of the SSQ. The best results were obtained when η was fitted independently. The VG-M and VG-B models produced reasonable fits, but their SSQ was of about an order of magnitude larger. Using BC-M and BC-B models we were unable to find a reasonable fit.

The BC- η functions (figure 3a, b) gave the smallest SSQ, producing cumulative infiltration curves very close to the measured ones (figure 2a).

4.2. SAND WITH MACROPORES

The double-porosity model requires the knowledge of hydraulic functions both for sand matrix and for the macropore system. For the sand matrix we used the previously identified BC- η functions. For the macropores we assumed step-like retention and conductivity functions. This was achieved using BC- η model with $\lambda = 7$ and $\eta = 7$, forcing $S_E(h)$ and $K(h)$ to tend to zero rapidly for $h < h_a$. We also assumed that $\theta_R = 0$ and $\theta_S = 1$. The theoretical values of the air-entry pressure and the conductivity at saturation can be calculated from the Laplace law and the Poiseuille law, i.e., $h_a = -0.149/\xi_1 = -1.5$ cm and $K_{S,2} = \rho g(\xi_1)^2/(8\mu) = 122.6$ cm s⁻¹, respectively, where ξ_1 – the macropore radius, ρ – the water density, g – the gravitational acceleration and μ – the water dynamic viscosity. However, using these values resulted in a very large overestimation of the infiltration rate. Thus we decided to identify h_a and K_S based on an inverse approach, while keeping the other parameters constant. The values obtained by numerical optimization are $h_a = -0.48$ cm and $K_S = 4.34$ cm s⁻¹, with SSQ = 9.71×10^4 cm⁶. In figures 3a,b, we present the fitted retention and conductivity functions of the macropores as well as the effective conductivity of the double-porosity medium in horizontal and vertical directions, calculated from equations (4a,b). Note that the macropores practically do not alter the medium conductivity in horizontal direction, while they significantly increase the vertical conductivity close to saturation. In figure 2b, the fitted cumulative infiltration curves for sand with macropores are compared with the experimental results.

5. CONCLUSIONS

The hydraulic functions indispensable to the double-porosity model were successfully identified using numerical inverse analysis. In particular, the increased infiltration rate for $h_{\text{surf}} = 0$ is well represented using the fitted parameters. The discrepancy between the theoretical and fitted values of h_a and K_S for macropores can be attributed to partial clogging of the macropores with sand, which reduces their diameter and increases the irregularity of the lateral surface.

ACKNOWLEDGEMENTS

This research was performed in the framework of the ECCO/PNRH Program “Transferts complexes en milieu poreux et ressources en eau” (INSU-CNRS).

REFERENCES

- [1] BROOKS R., COREY A., *Hydraulic properties of porous media*, Hydrology Paper No. 3, Colorado State University, Fort Collins, 1964.
- [2] BURDINE N., *Relative permeability calculations from pore size distribution data*, Petrol. Trans. Am. Inst. Min. Eng., 1953, 198, 71–77.
- [3] LEWANDOWSKA J., SZYMKIEWICZ A., BURZYŃSKI K., VAUCLIN M., *Modelling of unsaturated water flow in double porosity soils by the homogenization approach*, Adv. Water Resour., 2004, 27, 283–296.
- [4] LEWANDOWSKA J., SZYMKIEWICZ A., BOUTIN C., *Modelling of unsaturated hydraulic conductivity of double porosity soils*, Actes de 17ème Congrès Français de Mécanique, Troyes, Sept. 2005.
- [5] LUTZ P., *Influence des macropores sur l'infiltration d'eau dans les sols non saturés: caractérisation hydrodynamique par infiltrométrie sous pression contrôlée*, Memoire de DEA, Université Joseph Fourier, 1998, Laboratoire d'étude des Transferts en Hydrologie et Environnement, 46 p.
- [6] MUALEM Y., *A new model for predicting the hydraulic conductivity of unsaturated porous media*, Water Resour. Res., 1976, 12, 513–522.
- [7] PRESS W.H., FLANNERY B.P., TEUKOLSKY S.A., VETTERLING W.T., *Numerical recipes in Fortran*, Cambridge University Press, 1992.
- [8] RICHARDS L.A., *Capillary conduction of liquids through porous medium*, Physics, 1931, 1, 318–333.
- [9] SZYMKIEWICZ A., LEWANDOWSKA J., *Unified macroscopic model for unsaturated water flow in soils of bimodal porosity*, Hydrological Sciences Journal, 2006, 51, 1106–1124.
- [10] SZYMKIEWICZ A., LEWANDOWSKA J., ANGULO-JARAMILLO R., BUTLAŃSKA J., *Two-scale modeling of unsaturated water flow in the double-porosity medium under axi-symmetrical conditions*, 2007, submitted.
- [11] Van GENUCHTEN M.Th., *A closed form equation for predicting the hydraulic conductivity of unsaturated soils*, Soil Sci. Soc. Am. J., 1980, 44, 892–898.